Spatially resolved measurement of nonequilibrium quasiparticle relaxation in superconducting Al

K. Yu. Arutyunov,[1,2,*] H.-P. Auraneva,[1] and A. S. Vasenko[3,4,5]

[1]*University of Jyväskylä, Department of Physics, NanoScience Centre, PB 35, FIN-40014 Jyväskylä, Finland*

[2]*Nuclear Physics Institute, Moscow State University, 119992 Moscow, Russia*

[3]*Institut Laue-Langevin, 6 rue Jules Horowitz, BP 156, F-38042 Grenoble, France*

[4]*LPMMC, Université Joseph Fourier and CNRS, 25 Avenue des Martyrs, BP 166, F-38042 Grenoble, France*

[5]*Donostia International Physics Center (DIPC), Manuel de Lardizbal 5, E-20018 San Sebastián, Spain*

(Received 27 January 2011; published 18 March 2011)

Spatially resolved relaxation of nonequilibrium quasiparticles in a superconductor at ultralow temperatures was experimentally studied. It was found that the quasiparticle injection through a tunnel junction results in the modification of the shape of the I-V characteristic of a remote "detector" junction. The effect depends on the temperature, injection current, and proximity to the injector. The phenomena can be understood in terms of the creation of quasiparticle charge and energy disequilibrium characterized by two different length scales $\Lambda_{Q^*} \sim 5$ and $\Lambda_{T^*} \sim 40$ μm. The findings are in good agreement with existing phenomenological models, while more elaborate microscopic theory is mandatory for a detailed quantitative comparison with the experiment. The results are of fundamental importance for understanding electron transport phenomena in various nanoelectronic circuits.

DOI: 10.1103/PhysRevB.83.104509 PACS number(s): 74.78.−w, 74.45.+c, 74.50.+r, 74.81.Bd

I. INTRODUCTION

The conversion of electric current at an interface between different materials is a common process in any electric circuit. At nanoscales the whole system might behave as an interface if the dimension(s) are comparable to the characteristic relaxation length. Of particular interest are boundaries with a superconductor where electric current converts from single electrons to Cooper pairs. In a superconductor at a finite temperature there are always nonpaired electrons called *equilibrium* quasiparticles. In the presence of additional disturbance their concentration can be increased by *nonequilibrium* quasiparticles. If these excitations originate solely from pair breaking they equally populate excitation spectrum with momenta $p_Q > p_F$ (electron-like) and $p_Q < p_F$ (hole-like), where p_F is the Fermi momentum. Such a perturbation contributes to the *longitudinal* (or energy) mode (L) contrary to the *transverse* (or charge imbalance) mode (T) where the two branches of the excitation spectrum are nonequally populated.[1] Within the Keldysh formalism one can define the nonequilibrium distribution functions $f_{L,T}$ (Ref. 2). The usual electron distribution function is $2f = 1 - f_L - f_T$.

These phenomena attracted attention in the mid-1970s resulting in an impressive number of papers.[3,4] Those early experiments were mainly performed on sandwich-type flat structures not adequate for spatially resolved studies. Agreement between the experiment and theory was established reliably, mainly in the high temperature limit $T \to T_c$. The opposite limit $T \ll T_c$ has been poorly investigated. Recently the interest in the problem increased,[5–8] while the understanding is still far from being satisfactory. In addition to the general interest in physics of superconductivity, relaxation of quasiparticle excitations is a bottleneck process in many nanoelectronic applications: solid state coolers,[9–11] cold/hot electron bolometers,[12] and Cooper pair boxes.[13] Experimental study of the corresponding phenomena is the subject of the paper.

The paper is organized as follows. In the next section, we describe our setup and the experimental conditions. In Sec. III we discuss our experimental data. We also formulate a phenomenological model which is in a good agreement with our findings. The model enables us to obtain the energy and charge modes relaxation lengths. Finally, we summarize the results in Sec. IV.

II. EXPERIMENT

Multiterminal nanostructures (Fig. 1) were fabricated using electron beam lithography and ultra high vacuum evaporation of aluminum (S) and copper (N) separated by naturally grown aluminum oxide (I). The sample layout is conceptually close to the layout, described in Refs. 5 and 14. Electrons were injected into the superconductor through a large-area normal-insulator-superconductor (NIS) injector with typical tunnel resistance $\sim$3 kΩ. The induced disequilibrium was measured by remote detector NIS junctions with typical tunnel resistance $\sim$50 kΩ. Even at the lowest values of the utilized tunnel resistances one can neglect the proximity effect.

The ^{3}He^{4}He dilution refrigerator was located inside the electromagnetically shielded room with only battery-powered analog pre-amplifiers inside. A typical measuring setup (Fig. 1, top panel) consisted of two circuits: injector and detector. For detection two complementary configurations were used: either a single NIS junction, or two NIS junctions connected in series (NISIN) from both sides of the superconductor. The latter was found to be less sensitive to dc offsets presumably originating from parasitic thermoelectric effects. Care was taken not to increase the temperature of the system by the Joule heating at the injector by making the electrode rather massive (Fig. 1, bottom panel). An extra NIS junction (marked "Thermometer" in Fig. 1 and located $\simeq 1$ μm away from the injector junction) was used to measure the electron temperature of the injector $T_e^i(I_i)$ by fitting the experimental $I_T(V_T, I_i = \text{const})$ dependencies with the textbook expression for the tunnel current of a NIS junction. Here and below $I_i(V_i)$, $I_d(V_d)$, and $I_T(V_T)$ are the I-V characteristics of the injector, detector, and thermometer tunnel junctions, respectively (see

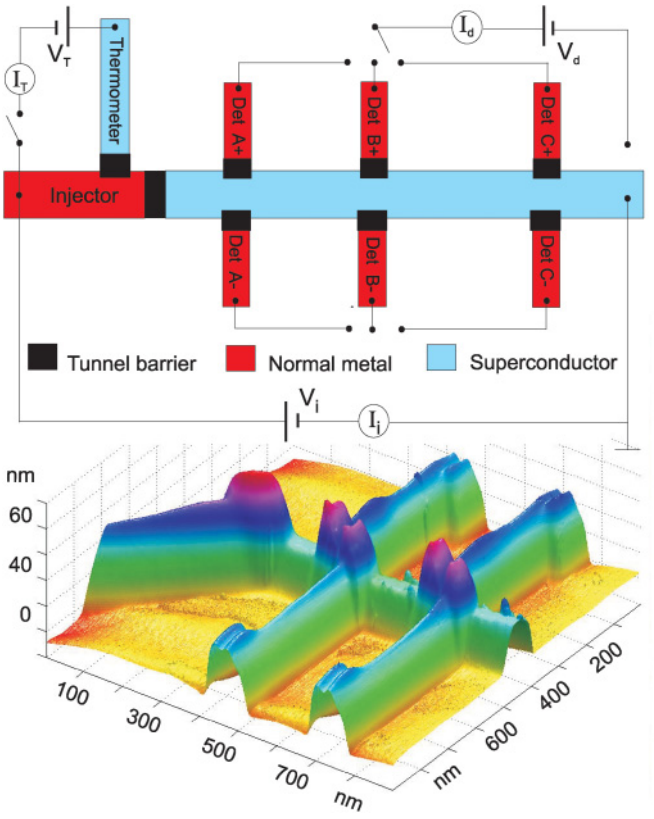

FIG. 1. (Color online) Top: schematics of the sample and measurements. Electron temperature of the normal metal injector is measured with the NIS junction "Thermometer." The quasiparticle relaxation in the superconducting long bar is determined by the "Detectors": either a single NIS junction, or a pair of connected in series NISIN junctions from the opposite sides of the superconductor. Bottom: scanning probe microscope image of the Si/SiO_x substrate with two closest detector pairs and the injector (left most massive probe). Typical thickness of the aluminum wire, copper detectors, and injector are 25, 40, and 80 nm, and the width 400, 180, and 1600 nm, respectively. Critical temperature of the aluminum wire is about 1.35 K and the low temperature mean free path $\ell \simeq 20$ nm.

Fig. 1, top panel). Once the relation $T_e^i(I_i, T = \text{const})$ was established, the corresponding "Thermometer" circuit was disconnected for the rest of the experiments.

III. RESULTS AND DISCUSSION

To avoid confusion it is instructive to summarize the definitions of various parameters of the dimensionality "temperature" hereafter used in the paper. The T stands for the bath temperature of the system measured by the two RuO_x resistors thermally anchored to the mixing chamber and the massive copper sample holder. The RuO_x sensors were calibrated against the nuclear orientation thermometer, and during the experiments their readings differ less than by a few mK.

The T_e^i and T_e^d denote the electron temperatures of the normal metal injector and detectors, respectively. The T_e^i and T_e^d are determined by fitting the corresponding $I_i(V_i)$ and $I_d(V_d)$ experimental dependencies by the well-known equilibrium expression for the tunnel current of a NIS junction. The T_e^i depends on the injection current, $T_e^i(I_i)$, due to the trivial Joule heating of the normal metal injector. At the lowest bath temperature $T \simeq 20$ mK and the highest injection currents $I_i \simeq 1\ \mu A$ the electron temperature of the injector increased by $\delta T_e^i \equiv T_e^i - T \simeq 100$ mK. The electron-phonon interaction is rather weak at ultralow temperatures,[9] and the superconducting "body" of the sample, thermally anchored to the substrate, has low thermal conductivity. Hence, the phonon temperature of the remote detectors should not deviate significantly from the bath temperature T. On the contrary, the electron temperature T_e^d of the normal detectors, determined by fitting the zero-injection $I_d(V_d, I_i = 0)$ dependency, was always higher than the base temperature T. The effect originates from the poor thermal coupling typical for ultralow temperatures and from the inevitable electron heating coming from the noisy electromagnetic environment. At a base temperature $T \simeq 20$ mK and zero injection $I_i = 0$ the absolute value of the detector electron temperature offset $\delta T_e^d \equiv T_e^d - T$ varied from 10 to 40 mK depending on the coupling of the particular junction with the measuring circuit. As the detectors are decoupled by the two NIS junctions from the remote "hot" injector, it is reasonable to assume that for the given detector its electron temperature T_e^d should not depend on the injection current I_i: $T_e^d(I_i > 0, T) \simeq T_e^d(I_i = 0, T)$.

The T_e^S denote the superconductor electron temperature. Formally, it should be determined taking into account a complicated energy balance.[9] From the very basic considerations one may expect that at nonzero quasiparticle injections $I_i > 0$ the actual (thermodynamic) temperature of the superconductor T_e^S, which enters into the nonequilibrium distribution function $f_T^S(E, T_e^S)$, should be higher than the bath temperature T. However, within the phenomenological formalism employed in the paper, T_e^S cannot be determined. More elaborate microscopic analysis (to our best knowledge, currently absent) should be used to determine the nonequilibrium (and essentially asymmetric with respect to the chemical potential) distribution function. Otherwise, any arbitrary value of T_e^S substituted into a symmetric (e.g., equilibrium) distribution function $f_T^S(E, T_e^S)$ gives exactly the same tunnel current of a NIS junction.

Finally, the T^* characterizes the reduction of the superconducting gap Δ. When the superconducting gap is suppressed by the quasiparticle injection one can use two complementary descriptions: either to deal with the bare experimental data $\Delta(I_i)$, or to convert the nonequilibrium energy gap into an effective temperature T^* using conventional (equilibrium) BCS expression. In the latter case T^* just means what would be the equilibrium temperature of the superconductor $T = T^*$ resulting in the corresponding reduction of the gap $\Delta(T_e^S, I_i > 0) = \Delta_{\rm BCS}(T^*, I_i = 0)$. It should be emphasized that T^* is only a convenient parameter of dimensionality "temperature" and has no direct relation to the (nonequilibrium) thermodynamic temperature T_e^S. As it will be shown below, the impact of quasiparticle injection on a superconductor is manifold. In particular, the longitudinal (energy) mode cannot be described solely by the reduction of the gap, or alternatively, the effective temperature T^*.

The injection of nonequilibrium quasiparticles into a superconductor results in a deviation of its density of states (DOS) N_S and distribution functions $f_{L,T}^S$ from equilibrium. Under certain assumptions the distribution function can be

found by deconvolution of the tunneling I-V dependencies.[15] In more general cases, a self-consistent solution of Keldysh-Usadel equations is required.[2] For the interpretation of the results we take the simplified approach *postulating* equilibrium functional forms of the DOS and distribution function f_S, but with parameters deviating from their equilibrium values,

$$N_S(E,\Delta,\Gamma) = |\mathrm{Re}\{(E+i\Gamma/2)/\sqrt{(E+i\Gamma/2)^2-\Delta^2}\}|, \quad (1)$$

$$f_S\left(E,T_e^S,\mu^*\right) = 1/\left\{\exp\left((E-\mu^*)/k_BT_e^S\right)+1\right\}. \quad (2)$$

The deviation of f_L^S from equilibrium formally corresponds to an increase of T_e^S above the bath temperature T, while the deviation of f_T^S corresponds to a nonzero shift of chemical potential μ^*. Considering the above expression for f_S with two parameters, T_e^S and μ^*, one might account for both the longitudinal and the transverse mode excitations. For the analysis of the experimental data we utilized the simplified phenomenological approach with three fitting parameters: DOS broadening Γ (Ref. 16), superconducting gap Δ, and effective quasiparticle chemical potential μ^* (Refs. 17 and 18). All parameters can be defined by fitting experimental $I_d(V_d)$ and/or dI_d/dV_d dependencies. It should be noted that the utilized phenomenological analysis, based on the postulated equilibrium functional form of the distribution function $f_S(E,T_e^S,\mu^*)$, disables determination of the (thermodynamic) temperature of the superconductor T_e^S. A more elaborate model (to our best knowledge currently missing) is mandatory to deduce the nonequilibrium $f_S(E,T_e^S,\mu^*)$ and the corresponding T_e^S.

As the injected nonequilibrium quasiparticles relax on a certain length, the fitting parameters should depend on the injection rate (energy eV_i or current $I_i = V_iG_{NN}^i$) and the distance between the detector and the injector L_{id}. The $I_d(V_d)$ dependency of a NIS detector in the presence of nonequilibrium injection is

$$I_d = \left(G_{NN}^d/e\right)\int_0^\infty N_S(E,\Delta,\Gamma)\left[f_T^N - f_T^S\right]dE, \quad (3)$$

where G_{NN}^d is the normal state conductivity of the junction, $f_T^N(E,V_d,T_e^N) = \tanh\left((E+eV_d)/2k_BT_e^N\right) - \tanh\left((E-eV_d)/2k_BT_e^N\right)$ the equilibrium value of f_T in the normal detector, and $f_T^S(E,L_{id},T_e^S)$ the local nonequilibrium value of f_T in the superconductor. The first term corresponds to the textbook equilibrium expression for a NIS tunnel current, explicitly depending on properties of the superconductor only through its DOS $N_S(E,\Delta,\Gamma)$.

The shape of the experimental $I_d(V_d)$ characteristic depends on the quasiparticle injection (Fig. 2). By fitting $I_d(V_d)$ and/or dI_d/dV_d dependencies one finds that the parameters Γ and Δ depend on the injection rate, proximity to the injector L_{id}, and temperature T (Figs. 3 and 4). The smearing of the $I_d(V_d)$ dependence [rounding of the "corners" at $eV_d \simeq \Delta(I_i)$] can be assigned to the parameter $\Gamma(I_i)$ which enters the superconductor DOS and is physically related to the finite quasiparticle lifetime.[16] For the same injection rate I_i the temperature dependence $\Gamma(T,\ I_i = \mathrm{const},\ L_{id} = \mathrm{const})$ (right inset in Fig. 3) most probably originates from the more intensive relaxation of the quasiparticles (i.e., from the reduction of the quasiparticle lifetime responsible for finite Γ) due to inelastic scattering on phonons. The total number of quasiparticles entering the superconductor per unit time is proportional to I_i, while only the fraction $\sim\exp(-L_{id}/\sqrt{D\tau_R})$ reaches the detector. At low temperatures the recombination time τ_R can be estimated from the relation $\tau_0/\tau_R \sim (T/T_c)^{1/2}\exp(-\Delta/k_BT)$ with τ_0 being the electron-phonon scattering time.[19,20] These simple arguments qualitatively explain the spatial, energy, and temperature dependencies of Γ (Fig. 3), while a more elaborate model, presumably incorporating the effect of the environment,[21] is required for a quantitative analysis.

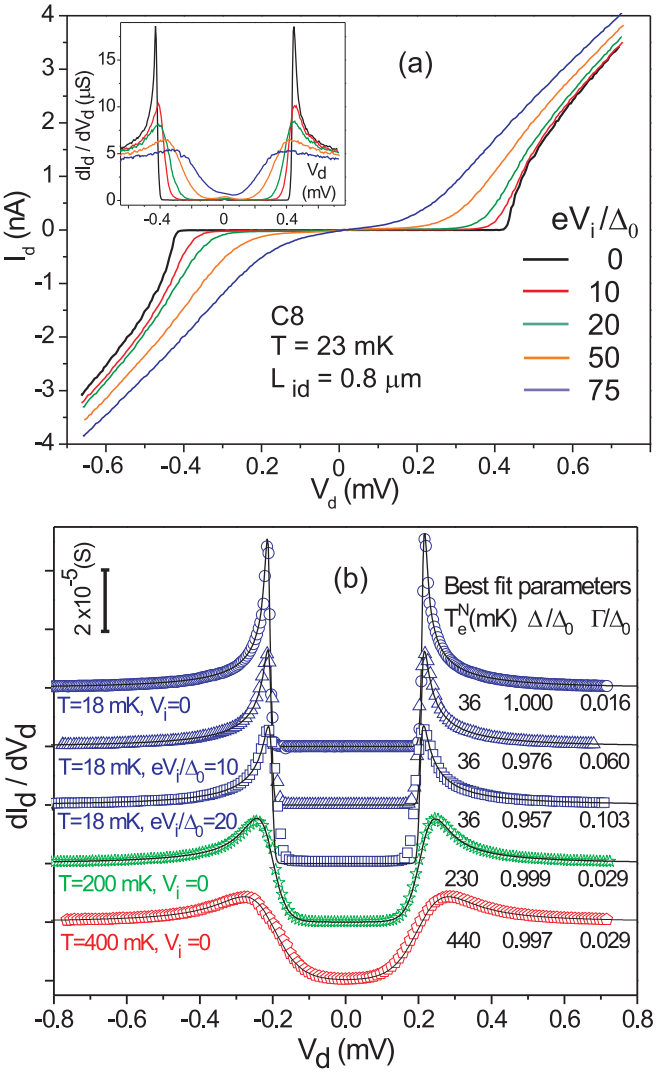

FIG. 2. (Color online) (a) Sample C8 $I_d(V_d)$ characteristics at various injections for the double junction NISIN detector located at $L_{id} = 0.8$ μm away from the injector. Inset: the corresponding dI_d/dV_d dependencies. Slight asymmetry of the dI_d/dV_d at high injections presumably originates from the not perfect equality of the each of the NIS junctions connetced in series. (b) Sample C2 NIS detector located at $L_{id} = 2.8$ μm experimental dI_d/dV_d dependencies at $T = 18 \pm 1$ mK at three injections $eV_i/\Delta_i = 0$ (◯), 10 (△), and 20 (□), and at $T = 200$ (★) and $T = 400$ (◇) mK at zero injections. Solid lines are the theoretical best fits with the fitting parameters indicated in the plot.

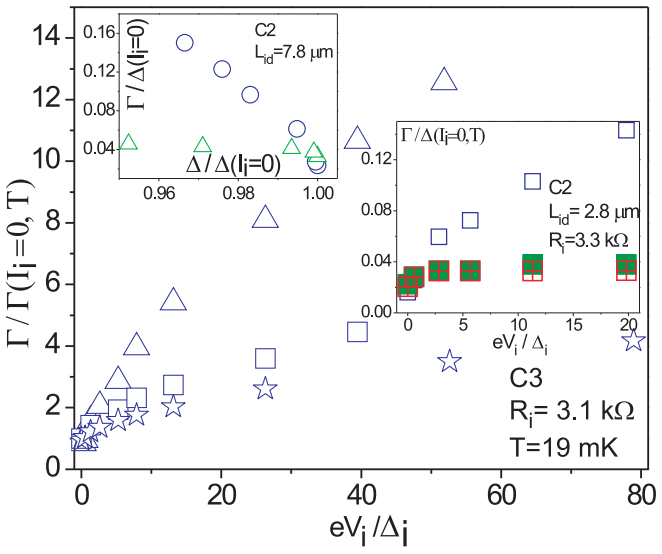

FIG. 3. (Color online) Depairing parameter Γ vs. injection energy for three detectors at $L_{id} = 0.8$ (△), 2.8 (□), and 7.8 (★) μm. Left inset: sample C2 NIS detector located at $L_{id} = 7.8$ μm $\Gamma(I_i)$ vs. $\Delta(I_i)$ at various injection currents I_i at $T = 18$ mK (◯) and $T = 200$ mK (△). Right inset: sample C2 Γ vs. injection energy at $L_{id} = 2.8$ μm at $T = 17.5$ (□), 200 (■), and 400 mK (⊞).

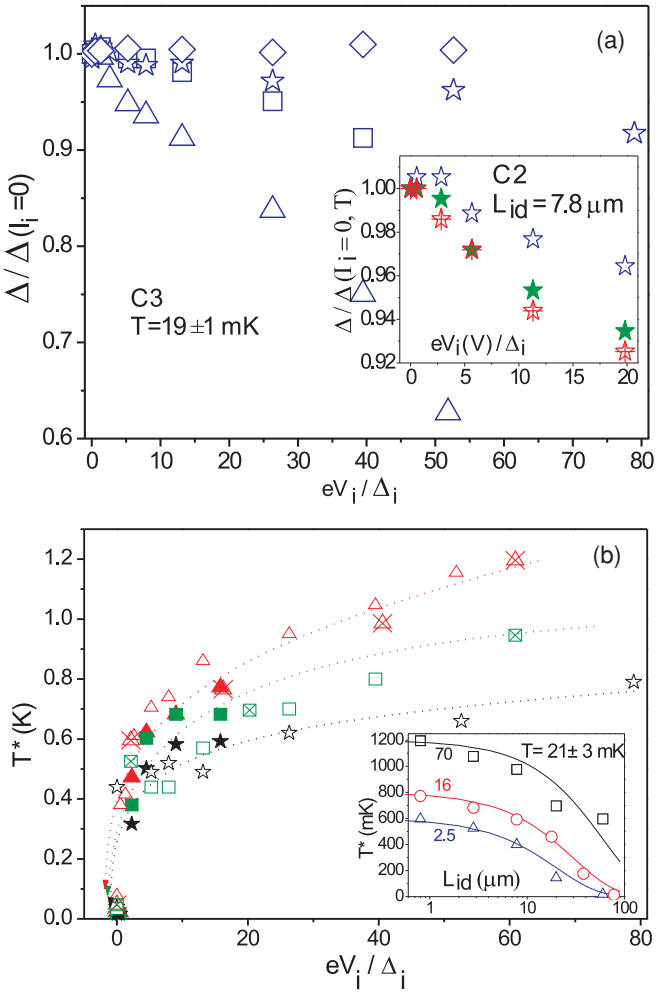

FIG. 4. (Color online) (a) Superconducting gap Δ vs. injection energy at $L_{id} = 0.8$ (△), 2.8 (□), 7.8 (★), and 17.8 (◇) μm. Inset: reduction of the superconducting gap measured by the same NIS detector at $L_{id} = 7.8$ μm at $T = 17.5$ (open star), 200 (★), and 400 (crossed star) mK. (b) Effective temperature T^* vs. injection energy for samples C3 (18 mK, open symbols), C2 (19 mK, solid symbols), and C8 (24 mK, crossed symbols) at $L_{id} = 0.8$ (△), 2.8 (□), and 7.8 (★) μm. Lines are guides to the eye. Inset: spatial decay of T^* averaged over several samples at $eV_i/\Delta_i = 70$ (□), 16 (◯), and 2.5 (△). Lines are fits assuming exponential dependence $\sim \exp(-L_{id}/\Lambda_{T^*})$.

Neglecting the superconducting phase, the gap equation for the pairing potential Δ, to be solved self-consistently with the Keldysh-Usadel equations, is $\Delta = \lambda \int_0^\infty f_L^S(E,L_{id})\mathrm{Re}(F)dE$, where λ is the electron-phonon coupling constant, F the anomalous pair amplitude, and $f_L^S(E,L_{id})$ the local nonequilibrium value of f_L in the superconductor.[2] At any energy E the function $f_L^S(E,L_{id})$ is smaller than its equilibrium value $\tanh(E/2k_BT)$ (Ref. 22), reducing Δ [Fig. 4(a)]. The effect is smaller at the lowest temperatures and increases with increasing bath temperature [Fig. 4(a), inset]. Utilizing the well-known BCS temperature dependence for the superconducting gap one can assign an effective temperature T^*, which would provide the same effect on the energy gap as the quasiparticle injection: $\Delta(T_e^S, I_i, L_{id}) = \Delta_{\mathrm{BCS}}(T^*, I_i = 0, L_{id})$ [Fig. 4(b)]. Assuming an exponential decay $T^* = T^*(0)\exp(-L_{id}/\Lambda_{T^*})$ one finds the characteristic length $\Lambda_{T^*} = 40$ μm ± 20 μm [Fig. 4(b), inset]. The large uncertainty comes from the weak $\Delta_{\mathrm{BCS}}(T)$ dependence at low temperatures and the limited set of L_{id} points (number of detectors). Once again we would like to remind that T^* is a convenient parameter introduced to account for the reduction of the superconducting gap $\Delta(I_i)$ and has no direct relation to the thermodynamic temperature of the superconductor T_e^S which should enter the corresponding nonequilibrium distribution function. It might even happen that in the limit of strong injection and weak quasiparticle-quasiparticle scattering T_e^S cannot be defined at all, while the nonequilibrium energy gap $\Delta(I_i)$, or alternatively $T^*(I_i)$, can be still deduced from the experimental $I_d(V_d)$ characteristics.

We believe that the reduction of the gap $\Delta(I_i)$ and the increase of $\Gamma(I_i)$ are the two manifestations of the same phenomenon—energy disbalance (longitudinal mode) accompanying injection of the nonequilibrium quasiparticles. Presumably, in a comprehensive microscopic description (to our best knowledge, currently missing) the longitudinal and the transverse modes may be entangled both contributing to the $\Delta(I_i)$ and $\Gamma(I_i)$ dependencies. Within the "orthodox" BCS model the (temperature-dependent) smearing of a NIS detector $I_d(V_d)$ characteristic comes solely from the distribution function of the normal electrode $f^N(E,V_d,T_e^N)$ and not from the DOS or distribution function of the superconductor. The temperature of the superconductor T_e^S enters solely through the temperature dependence of the gap $\Delta(T_e^S)$. In a typical equilibrium situation $T = T_e^N = T_e^S$. Employed in the paper analysis deviates from that "orthodox" model by introduction of the Dynes smearing $\Gamma[I_i]$ entering the DOS of the superconductor $N_S(E,\Delta[I_i],\Gamma[I_i])$, Eq. (1), at a given, but not defined, temperature of the superconductor T_e^S, which

indeed leads to the extra (nontemperature dependent) smearing of the $I_d(V_d)$ dependence, Eq. (3).

The employed analysis of the experimental data based on the equilibrium expression for the tunnel current [first term in Eq. (3)] with the DOS deviating from the "orthodox" BCS model [Eqs. (1) and (2)] enables separation of the two impacts $\Delta(I_i)$ and $\Gamma(I_i)$. The reduction of the gap $\Delta(I_i)$ (Fig. 4) leads to a "sharp" $I_d(V_d)$ characteristic: as if the temperature is still low $T_e^S \simeq T$, but the energy gap is reduced $\Delta(I_i > 0) < \Delta(I_i = 0)$. The impact of the finite $\Gamma(I_i)$ manifests itself as the smearing of the $I_d(V_d)$ characteristics at the "corners" $eV_d \simeq \pm\Delta(I_i)$ which cannot be accounted for any reasonable value of T_e^N.

It is important to emphasize that the experimental nonequilibrium $I_d(V_d, I_i > 0, T)$ dependencies cannot be described by the "orthodox" BCS model just assuming that the temperature of the system has increased above the bath temperature: $T \to T_e^N, T_e^S \gg T$. At $T \ll T_c$ the shape of the experimental $I_d(V_d, I_i > 0, T)$ characteristics is qualitatively different from the reference equilibrium characteristics $I_d(V_d, I_i = 0, T')$ taken at elevated temperatures $T' > T$ [Fig. 2(b)]. Those zero-injection high-temperature $I_d(V_d)$ characteristics can be nicely fit by the equilibrium BCS expression for the tunnel current [first term in Eq. (3)] assuming small intrinsic Dynes broadening of the DOS, Eq. (1), with $\Gamma(I_i = 0)/\Delta(I_i = 0) \simeq 0.02$ [Fig. 2(b)] in a reasonable agreement with the existing data on aluminum.[21] However, one runs into a contradiction trying to fit the experimental $I_d(V_d, I_i > 0, T)$ characteristics using a single fitting parameter $T_{\rm fit}$ and the first term in the expression (3) for the NIS tunnel current. To properly account for the gap reduction $\Delta(I_i)$ one should set the best fit "equilibrium" temperature $T_{\rm fit} = T^* \gg T$ [compare Figs. 2(b) and 4(b)] being significantly higher than the temperature of the "hottest" part of the system—the injector. While to account for the observed broadening at the gap edge, the effective fitting temperature $T_{\rm fit}$ should be set significantly lower $T_{\rm fit} \simeq T_N^e \ll T^*$ [Fig. 2(b)]. Summarizing, one should conclude that at nonzero injections the $I_d(V_d, I_i > 0, T)$ characteristics cannot be described by a single "equilibrium" temperature $T_{\rm fit}$. The two independent parameters, $\Delta(I_i)$ and $\Gamma(I_i)$, are necessary. The dependencies $\Delta(I_i)$ and $\Gamma(I_i)$ on the injection rate are different. At ultralow temperatures $T \ll T_c$ and modest injections $eV_i/\Delta_0 \lesssim 10$ the suppression of the gap is rather small [Fig. 4(a)], while the increase of the DOS broadening parameter Γ is quite pronounced (Fig. 3). At elevated temperatures the dependence of Γ on the injection rate is rather weak (insets in Fig. 3). We would like to emphasize that the necessity to introduce the two independent parameters $\Delta(I_i)$ and $\Gamma(I_i)$ is the result of the employed phenomenological approach based on Eqs. (1) through (3). We would wish to believe that in an elaborated microscopic model dealing with the essentially nonequilibrium distribution function $f_S(E, T_e^S)$ a single parameter—the truly thermodynamic temperature of the superconductor T_e^S—would be sufficient to account for the whole variety of the experimental data.

A remarkable feature of the tunnel current expression is the existence of the nonzero excess current $I_d^{ex} = I_d(V_d = 0)$ originating from the independence of $f_T^S(E, L_{id}, T_e^S)$ on the bias volatage V_d [second term in Eq. (3)]. The effect has been observed in NISIS' flat sandwiches[23,24] and recently in multiterminal NIS structures.[5] Within our phenomenological approach, the experimentally measured excess current is linked to the effective quasiparticle chemical potential,[24] $I_d^{ex} = (G_{NN}^d/e)\mu^*$. A typical example of a NIS detector subgap $I_d(V_d)$ characteristic is shown in Fig. 5(a). The excess current increases with the increase of the injection rate reversing its sign with the change of the injection polarity. The effect decreases with increasing distance to the injector L_{id} [Fig. 5(b)] and the bath temperature [Fig. 5(c)]. Slight asymmetry of I_d^{ex} with respect to zero injection [Fig. 5(a)] probably originates from a parasitic residual thermo-electric potential. It should be noted that in the NISIN detector geometry the excess current is absent since the contributions from the two NIS junctions connected in series and located at the same distance L_{id} (from the opposite sides of the superconducting bar, see Fig. 1), cancel each other. The double NISIN junctions were used only as a complementary configuration in the experiments on the energy mode relaxation [Fig. 2(a)].

The solution of the diffusion equation for the charge imbalance Q^* gives the excess current

$$I_d^{ex} = I_i \frac{F^* \Lambda_{Q^*} G_{NN}^d}{2e^2 N(0) D\sigma} \exp(-L_{id}/\Lambda_{Q^*}), \tag{4}$$

where $N(0) = 1.08 \times 10^{47}\ 1/J \times {\rm m}^3$ is the normal state DOS for aluminium at the Fermi level, and F^* is a smooth function varying from 0 at no injection to 1 at $eV_i \gg \Delta_i$ (Ref. 24). Substituting the mean free path $\ell \simeq 20$ nm, Fermi velocity $v_F = 1.36 \times 10^6$ m/s, diffusivity $D = 1/3 v_F \ell$ and cross section $\sigma = 25\,{\rm nm} \times 400$ nm one gets an acceptable fit for the dependence of the excess current on the injection energy [Fig. 5(b)]. The best-fit charge imbalance length $\Lambda_{Q^*} = \sqrt{D\tau_{Q^*}}$ varies from 3.5 to 6.5 μm being in a reasonable agreement with recent findings.[5,8]

Weak temperature dependence of the charge imbalance relaxation $Q^* \sim I_d^{ex} \sim \mu^*$ [Fig. 5(c)] at ultralow temperatures is expected: In the absence of an effective electron-phonon interaction the remaining (weak) mechanism is the elastic scattering due to the gap inhomogeneity, and/or anisotropy or even just a finite supercurrent.[24] Contrary to the transverse mode relaxation, the relaxation of the longitudinal (energy) mode always requires the presence of inelastic mechanism(s). At the ultralow temperatures of the experiment $k_B T \ll \Delta$ there are very few equilibrium phonons capable of providing the quasiparticle energy relaxation. The only (potential) source of the phonons with energies above the bath temperature T is the Joule heating in the injector. However, how it has been already discussed, even in the worst-case scenario of the strongest injection the diffusion of heat from the "hot" injector into the superconductor, is not sufficient to account for our findings. The maximum rise of the electron temperature in the injector $\delta T_e^i \simeq 100$ mK. Even assuming a perfect electron-phonon coupling in the injector, the energy of the corresponding phonons is still much smaller than the energy $\geqslant 2\Delta$ required for a pair of hole-like and electron-like quasiparticles to form a Cooper pair. However, as the quasiparticle recombination finally does happen on "astronomically" large (for a superconductor) scales $\Lambda_{T^*} \simeq 40$ μm, some weak mechanism should exist. For example, emission/re-absorption of nonequilibrium

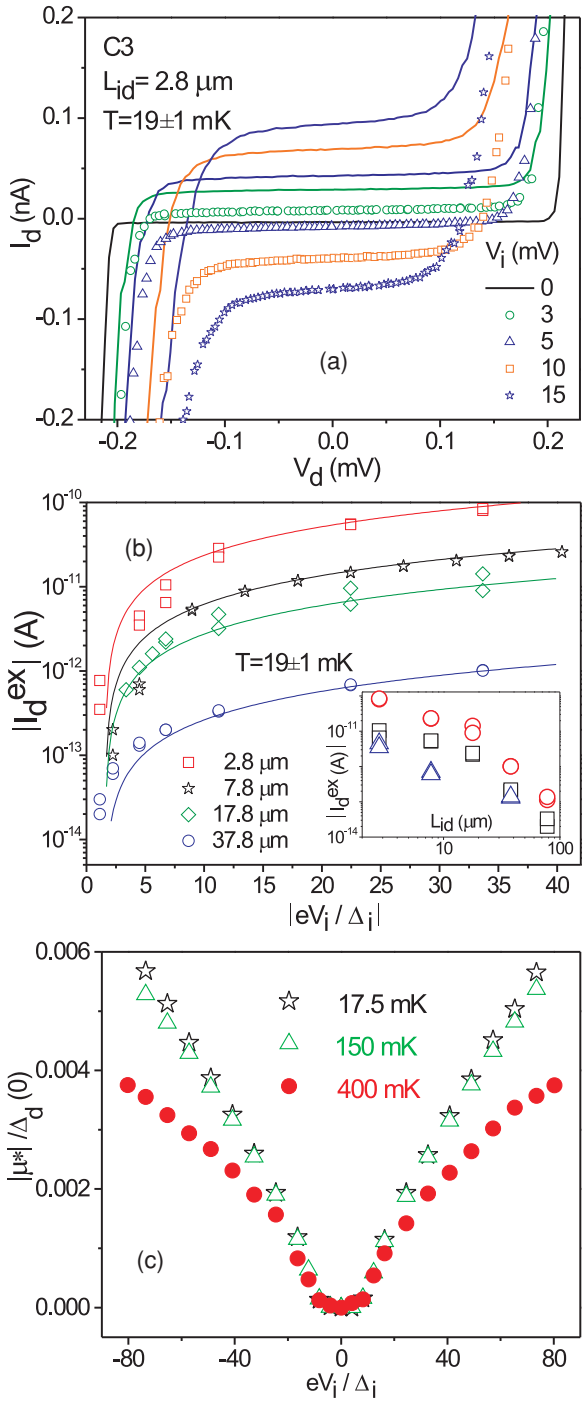

FIG. 5. (Color online) Sample C3 NIS detection. (a) Zoom of the subgap region of the $I_d(V_d)$ characteristic at different injection voltages $V_i = 0$, 3, 5, 10, and 15 mV. Lines correspond to the same injections of reverse polarity. (b) Excess current I_d^{ex} vs. injection energy eV_i/Δ_i at different distances L_{id}. Lines are fits utilizing $\Lambda_{Q^*} = 3.6, 3.6, 5.2$, and 6.4 μm for the detectors located at $L_{id} = 2.8$, 7.8, 17.8, and 37.8 μm, respectively. Inset: spatial decay of the excess current measured at $|\, eV_i/\Delta_i \,| = 33.7$ (◯), 6.7 (□), and 4.5(△). (c) Normalized chemical potential μ^* vs. injection energy measured at various temperatures by the same detector at $L_{id} = 7.8$ μm.

phonons or photons, might provide the required energy relaxation. Certainly, these mechanisms should also contribute to the relaxation of the transverse mode. The observation $\Lambda_{Q^*} < \Lambda_{T^*}$ supports our conclusion that at ultralow temperatures the elastic scattering is an important channel of the charge imbalance relaxation.

The substantial quantitative difference between Λ_{T^*} and Λ_{Q^*} at ultralow temperatures, $T \ll T_c$, is in qualitative agreement with previous calculations.[19,20] The explicit condition when one can neglect the elastic scattering has been obtained in Ref. 25, $(T_c - T)/T_c \ll (\tau_E T_c)^{-2/3}$, where τ_E is the energy relaxation time (measured in $1/K$). Analysis of this expression leads to the conclusion that the only physical limit when always $\Lambda_{Q^*} \gg \Lambda_E$ is at $T \to T_c$, where Λ_{Q^*} diverges. Formally, it means that in the normal state there is no branch relaxation mechanism. Our experiments were made at very low temperatures much smaller then T_c. At such low temperatures, to our best knowledge, there is no general criterion to *a priori* relate Λ_{Q^*} with Λ_{T^*}.

IV. CONCLUSION

In conclusion, we performed spatially resolved measurements of the nonequilibrium quasiparticle relaxation in superconducting aluminum at ultralow temperatures $T \ll T_c$. The analysis employs the phenomenological interpretation postulating equilibrium functional dependencies of DOS and the distribution function of the superconductor, while assuming that the broadening parameter Γ, effective chemical potential μ^*, and superconducting gap Δ depend on the rate of quasiparticle injection and the proximity to the injector. Two scales $\Lambda_{T^*} = 40 \pm 20$ and $\Lambda_{Q^*} = 5 \pm 1.5$ μm are responsible for the relaxation of the energy (longitudinal) and charge (transverse) modes, respectively. Both quantities were measured simultaneously in the same samples using the same experimental technique eliminating sample/measurement artifacts. This is the central result of the paper. It should be emphasized that both the energy and the charge disequilibrium are universal phenomena which should be taken into consideration in a broad class of systems involving electron[9–13] spin and/or coherent nonlocal[26] transport. Despite the reasonable agreement with the phenomenological description, the application of the relaxation approximation for the essentially spatially inhomogeneous problem is not fully justified at low temperatures $T \ll T_c$. A more elaborate microscopic model is required for a quantitative analysis. We hope that our findings will trigger the corresponding research activity.

ACKNOWLEDGMENTS

The authors would like to acknowledge the support of the TEKES project DEMAPP, FCPK Grant No. 2010-1.5-508-005-037, NanoSCIERA project Nanofridge, and ANR-DYCOSMA. We thank A. Julukian and L. Leino for AFM analysis, and D. Beckmann, E. Bezuglyui, D. Golubev, F. Hekking, N. Kopnin, and A. Zaikin for discussions. A.S.V. acknowledges the hospitality of Donostia International Physics Center (DIPS) during his stay in San Sebastián, Spain.

*konstantin.arutyunov@phys.jyu.fi

[1] A. Schmid and G. Schön, J. Low. Temp. Phys. **20**, 207 (1975).
[2] W. Belzig, F. K. Wilhelm, C. Bruder, G. Schön, and A. D. Zaikin, Superlatt. Microstruct. **25**, 1251 (1999).
[3] See for a comprehensive review, *Nonequlibrium Superconductivity, Phonons, and Kapitza Boundaries*, edited by K. E. Gray (Plenum Press, New York, 1981).
[4] See for a comprehensive review, N. B. Kopnin, *Theory of Nonequlibrium Superconductivity* (Oxford University Press, New York, 2001).
[5] R. Yagi, Superlattices Microstruct. **34**, 263 (2003); Y. Ikebuchi and R. Yagi, Physica E **22**, 757 (2004); R. Yagi, Phys. Rev. B **73**, 134507 (2006); R. Yagi, K. Tsuboi, R. Morimoto, T. Matsumura, and H. Kobara, J. Phys. Soc. Jpn. **78**, 054704 (2009).
[6] A. V. Timofeev, C. P. García, N. B. Kopnin, A. M. Savin, M. Meschke, F. Giazotto, and J. P. Pekola, Phys. Rev. Lett. **102**, 017003 (2009).
[7] N. B. Kopnin, Y. M. Galperin, J. Bergli, and V. M. Vinokur, Phys. Rev. B **80**, 134502 (2009).
[8] F. Hübler, J. C. Lemyre, D. Beckmann, and H. v. Löhneysen, Phys. Rev. B **81**, 184524 (2010).
[9] F. Giazotto, T. T. Heikkilä, A. Luukanen, A. M. Savin, and J. P. Pekola, Rev. Mod. Phys. **78**, 217 (2006).
[10] J. P. Pekola, A. J. Manninen, M. M. Leivo, K. Arutyunov, J. K. Suoknuuti, T. I. Suppula, and B. Collaudin, Physica B **280**, 485 (2000).
[11] A. S. Vasenko, E. V. Bezuglyi, H. Courtois, and F. W. J. Hekking, Phys. Rev. B **81**, 094513 (2010).
[12] L. Kuzmin, in *Proceedings of SPIE Astronomical Telescopes and Instrumentation Conf. Mm and Submm Detectors* 5498, 349-361 (2004).
[13] V. Bouchiat, D. Vion, P. Joyez, D. Esteve, and M. H. Devoret, Phys. Scr. T **76**, 165 (1998); J. Aumentado, M. W. Keller, J. M. Martinis, and M. H. Devoret, Phys. Rev. Lett. **92**, 066802 (2004); J. Mannik and J. E. Lukens, *ibid*. **92**, 057004 (2004).
[14] M. L. Yu and J. E. Mercereau, Phys. Rev. Lett. **28**, 1117 (1972); G. J. Dolan and L. D. Jackel, *ibid*. **39**, 1628 (1977).
[15] H. Pothier, S. Guéron, Norman O. Birge, D. Esteve, and M. H. Devoret, Phys. Rev. Lett. **79**, 3490 (1997); F. Pierre, A. Anthore, H. Pothier, C. Urbina, and D. Esteve, *ibid*. **86**, 1078 (2001).
[16] R. C. Dynes, V. Narayanamurti, and J. P. Garno, Phys. Rev. Lett. **41**, 1509 (1978); R. C. Dynes, J. P. Garno, G. B. Hertel, and T. P. Orlando, *ibid*. **53**, 2437 (1984).
[17] W. H. Parker, Phys. Rev. B **12**, 3667 (1975).
[18] C. S. Owen and D. J. Scalapino, Phys. Rev. Lett. **28**, 1559 (1972).
[19] S. B. Kaplan, C. C. Chi, D. N. Langenberg, J. J. Chang, S. Jafarey, and D. J. Scalapino, Phys. Rev. B **14**, 4854 (1976).
[20] C. C. Chi and J. Clarke, Phys. Rev. B **19**, 4495 (1979).
[21] J. P. Pekola, V. F. Maisi, S. Kafanov, N. Chekurov, A. Kemppinen, Yu. A. Pashkin, O.-P. Saira, M. Möttönen, and J. S. Tsai, Phys. Rev. Lett. **105**, 026803 (2010).
[22] A. S. Vasenko and F. W. J. Hekking, J. Low Temp. Phys. **154**, 221 (2009).
[23] J. Clarke, Phys. Rev. Lett. **28**, 1363 (1972).
[24] M. Tinkham and J. Clarke, Phys. Rev. Lett. **28**, 1366 (1972).
[25] E. V. Bezuglyi, E. N. Bratus', and V. P. Galaiko, Fiz. Nizk. Temp. **3**, 1010 (1977) [Sov. J. Low Temp. Phys. **3**, 491 (1977)].
[26] D. Beckmann, H. B. Weber, and H. v. Löhneysen, Phys. Rev. Lett. **93**, 197003 (2004); S. Russo, M. Kroug, T. M. Klapwijk, and A. F. Morpurgo, *ibid*. **95**, 027002 (2005); P. Cadden Zimansky and V. Chandrasekhar, *ibid*. **97**, 237003 (2006).